Progress In Electromagnetics Research, PIER 80, 197–224, 2008

METHOD OF EDGE CURRENTS FOR CALCULATING MUTUAL EXTERNAL INDUCTANCE IN A MICROSTRIP STRUCTURE

M. Y. Koledintseva, J. L. Drewniak, T. P. Van Doren D. J. Pommerenke and M. Cocchini

Electromagnetic Compatibility Laboratory
University of Missouri-Rolla
1870 Miner Circle, Rolla, MO 65409-0040, USA

D. M. Hockanson

Sun Microsystems, Inc.
901 San Antonio Road, Palo Alto, CA 94303, USA

Abstract—Mutual external inductance (MEI) associated with fringing magnetic fields in planar transmission lines is a cause of so-called "ground plane noise", which leads to radiation from printed circuit boards in high-speed electronic equipment. Herein, a *Method of Edge Currents (MEC)* is proposed for calculating the MEI associated with fringing magnetic fields that wrap the ground plane of a microstrip line. This method employs a quasi-magnetostatic approach and direct magnetic field integration, so the resultant MEI is frequency-independent. It is shown that when infinitely wide ground planes are cut to form ground planes of finite width, the residual surface currents on the tails that are cut off may be redistributed on the edges of the ground planes of finite thickness, forming edge currents. These edge currents shrink to filament currents when the thickness of the ground plane becomes negligible. It is shown that the mutual external inductance is determined by the magnetic flux produced by these edge currents, while the contributions to the magnetic flux by the currents from the signal trace and the finite-size ground plane completely compensate each other. This approach has been applied to estimating the mutual inductance for symmetrical and asymmetrical microstrip lines.

1. INTRODUCTION

Planar transmission lines are widely used in high-speed digital and analog electronic devices, from signal traces on printed circuit boards (PCB), to feeding networks in active and passive IC components. Nowadays, there are many books and papers on planar transmission line design and analysis of various intrinsic parameters of microstrip structures, such as their RLCG parameters (see e.g., [1–5] and references therein). There are also many publications in PIER and JEMWA on the design of complex functional devices on the basis of planar transmission lines, including those with multiple signal conductors, where the problem of signal coupling is the most important [6–13]. Microstrip structures with comparatively narrow ground planes (GP) have various applications in modern high-speed electronic equipment, for example, to increase product assembly density, for interboard connector design, or for microstrip on-chip interconnects on silicon [3, 14, 15]. A major problem in most of the structures with narrow ground planes, or when signal traces come close to the edge of a printed circuit board is so-called "*ground plane noise*", which is actually a *common-mode voltage*, that appears on the reference plane due to fringing magnetic fields wrapping the plane [16–21]. This voltage drives unintentional "antennas" formed by parts of the electronic equipment, such as PCB reference planes, cables, and the conducting chassis that are connected to the reference plane of the microstrip structures. The common-mode voltage is related to the differential-mode (signal) current in the trace at the same frequency [18]

$$V_{CM}(\omega) = Z_t \cdot I_{DM}(\omega), \tag{1}$$

where $Z_t \approx R_{gp} + j\omega M$ is the transfer impedance per unit length. If the ground plane resistance R_{gp} is negligible, then the transfer impedance is represented mainly by the mutual inductance M associated with fringing magnetic fields wrapping the ground plane. This inductance is further called the *mutual external inductance* (MEI).

Common-mode source identification and conducted emission calculations depend on the accuracy with which the above mutual inductance is known for the particular geometry — relative position of traces, vias, and signal return paths. At frequencies where the PCB structures must be modeled using distributed parameters, quantifying the inductive coupling mechanism is an important, but a difficult problem. Recently, there have been many publications aimed at this problem [16–24].

An analytical method of calculating the MEI associated with fringing magnetic fields in microstrip structures, both symmetrical

and asymmetrical, is represented in this paper. This method employs a quasi-magnetostatic approach, image theory and direct integration of the magnetic field, and is based on the concept of *edge currents*. These edge currents are formed, when an infinitely wide ground plane is cut to form a ground plane of finite width. Herein, it is shown that it is the edge currents that contribute mainly to the MEI of interest. The presented method can be applied to planar transmission line structures with many signal traces and many ground planes, too. The analysis of mutual external inductance related to the radiation of planar structures with finite-size ground planes can also be useful when designing microstrip patch antennas [25–31] and other radiating devices [32].

One of the approaches for estimating any inductance is calculating a ratio of the total magnetic flux penetrating through a well-defined loop to the amplitude of current that produces this flux. Unlike capacitance or resistance, inductance is always associated with a closed current loop. The MEI is defined here as the mutual inductance between the signal current loop and the common mode (CM) "antenna" current loop, as shown in Figure 1.

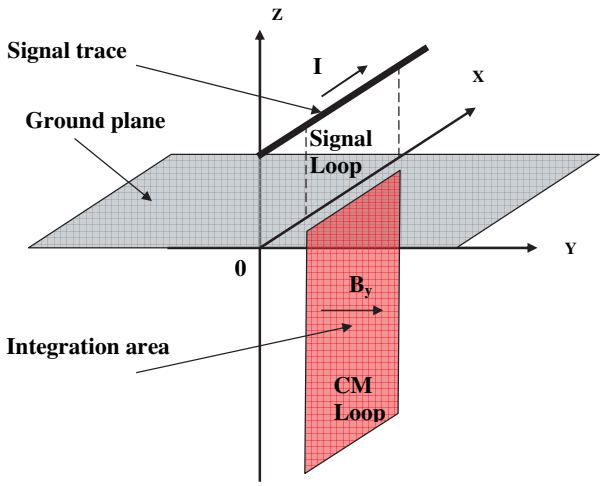

Figure 1. Differential- and common-mode current loops for determining the MEI associated with fringing magnetic fields in a microstrip geometry.

To define this inductance, assume that the ground plane is in the horizontal *(xy)* plane, and the signal trace is at $y = 0$. If the structure has a finite ground plane, but is infinite and homogeneous in the direction of wave propagation (x-direction), then the per-unit-

length (*p.u.l.*) mutual external inductance can be defined as

$$M_{p.u.l.} = \frac{\Psi}{I \cdot \ell_x} = \frac{1}{I} \cdot \int_z B_y dz, \tag{2}$$

where the integration is taken along the z-axis below the ground plane. Because of the translational invariance of the cross-sectional geometry along the x-axis, the integration along x in (2) is omitted. If the origin of the coordinate system is in the center of the ground plane of finite thickness d, then the integral is taken in the limits $z = (-\infty, -\frac{d}{2})$, and it must converge at both $z \to -\infty$ and $z \to -\frac{d}{2}$.

There are different ways to calculate the inductance of interest. The classical book by Grover [33] on inductance calculations describes many methods, such as the Newmann formula [34], energy conservation approaches developed by the classical physicists Faraday, Helmholtz, Thomson, and Maxwell, as well as Maxwell's Geometric Mean Distance (GMD) approach [35]. However, the GMD method is used mainly for symmetric finite geometries, and cannot be used for per-unit-length parameters, unless the assumption that the structure is infinitely long and translationally invariant is made. Conformal mapping and the complex potential method was developed by Kaden and applied to magnetic coupling in translationally invariant and infinitely long structures along one axis, with a non-uniform current distribution in the cross-sectional plane [36]. Kaden obtained an explicit formula for the mutual inductance of two filaments separated by a shield of finite width [36]. Grover's partial inductance approach for treating complex geometries was further developed by Ruehli [37], and splits a complex structure into filaments. Van Horck considers the mutual inductance between two signal traces shifted from the center and placed on different sides of a ground plane [16], using Carson's approach for calculating the return current distribution over a wide ground plane [38]. For a ground plane of finite size, closed-form expressions are available only for the microstrip case with either a non-shifted strip [16–20], or a strip shifted to the very edge of the ground plane [16]. Some papers contain numerical or simplified analytical evaluations of the ground plane internal impedance of microstrip lines using the quasistatic current density distribution in the ground plane produced by a signal trace [16, 18, 22, 39, 40]. Reference [23] contains a general dual integral approach for the analysis of the finite-size ground plane self-inductance of a microstrip, which takes into account wave propagation effects. However, there are only implicit expressions for inductance associated with the flux through the loop between the signal trace and the ground plane. Moreover, the resultant value

of inductance is frequency-dependent in principle, and it cannot be associated with a lumped-element analog.

The method proposed herein for calculating MEI for microstrip lines uses a quasi-magnetostatic approach and the *direct analytical calculation of the magnetic flux* penetrating through the desired loop area is considered. This approach is denoted the *Method of Edge Currents (MEC)*, since it will be shown below that only edge currents on the ground planes are responsible for the mutual inductance under study. It is known that this inductance gives rise to the radiation from cables due to the common-mode voltage associated with a finite size signal reference plane. The results of the computations obtained from the proposed method are compared with the literature results based on the Schwarz-Christoffel (SC) conformal mapping transformation [41], as well as some experimental data, and some results of full-wave numerical modeling fulfilled using the *CST Microwave Studio* (*CST MWS*) software. The external mutual inductance is found from the *CST MWS* calculations as

$$M_{p.u.l} = \mu_0 \sum_{i=1}^{N} \frac{H_0(z_i)}{I_{trace}} \Delta z_i = \mu_0 \sum_{i=1}^{N} 10^{\alpha_i/20} \Delta z_i, \tag{3}$$

where $H_0(z_i)$ is the magnitude of the magnetic field at the cross-section z_i, and the value $\alpha_i = 20 \cdot \log\left(\frac{H_0(z_i)}{I_{trace}}\right)$ is the corresponding magnetic probe magnitude, "measured" in dB. The "*p.u.l.*" subscript is omitted during further consideration. To assign (3) as a per-unit-length distributed element characteristic of a microstrip structure, it is necessary that this value be constant in the frequency range of interest, or at least at lower frequencies. The frequency is limited by the validity of the quasistatic approximation for the magnetic field, i.e., when the cross-sectional dimensions of the transmission line are at least one order smaller than the wavelength in the dielectric of the line, or when $E_x, H_x \approx 0$.

2. MODEL DESCRIPTION

The mutual external inductance associated with the fringing magnetic fields in a microstrip structure with a ground plane of finite size is considered in this Section. For the analytical considerations it is assumed that all the cross-sectional dimensions are much smaller than the wavelength of the electromagnetic field, so that a quasi-TEM approach is valid [13, 15]. The substrate in the microstrip line is a non-magnetic dielectric. The length of the transmission line is much greater

than the other dimensions, so that per-unit-length parameters can be calculated. Both the ground plane and a signal trace are assumed to be perfect electric conductors, so that no magnetic energy is stored within them, and image theory can be used. In the presented model, a finite thickness of the ground plane and a finite width of the signal trace are taken into account. Both symmetrical and asymmetrical (with non-centered signal trace) microstrip structures are studied.

2.1. Symmetrical Microstrip Structure

Let the microstrip geometry be translationally invariant along the x-axis, resulting in a two-dimensional (2D) cross-section as shown in Figure 2.

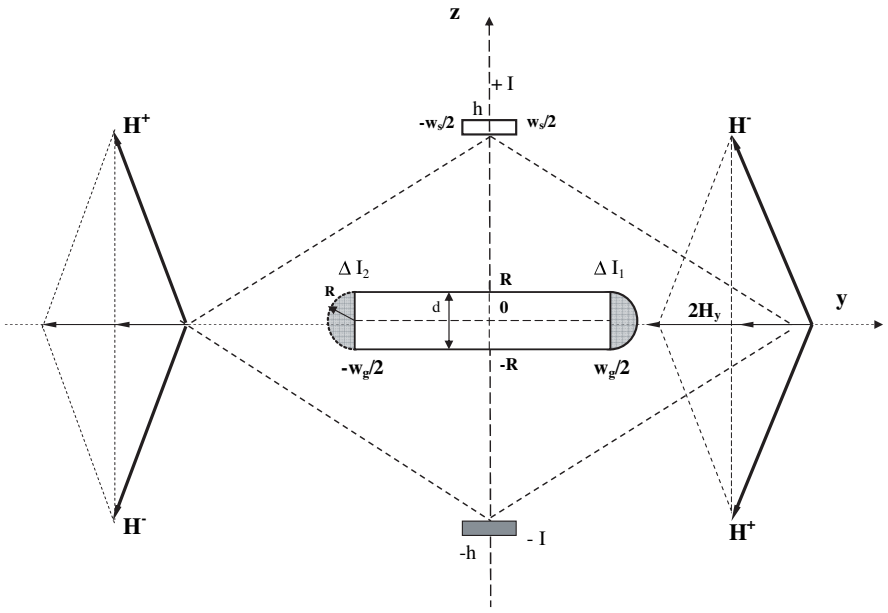

Figure 2. Application of image theory for the differential-mode and common-mode current loops mutual inductance extraction in the microstrip case.

First, for simplicity, let the microstrip signal trace be a thin filament. Initially assume that the ground plane is infinitely wide. For an infinite perfect electric conducting (PEC) ground plane, according to image theory, there are two sources $+I_S$ (initial current source) and $-I_S$ (image source). The initial and image sources produce equal

y-components of the static magnetic field along the y-axis given by Ampere circuital law,

$$H_y^{\pm} = \frac{I_S \cdot h}{2\pi(h^2 + y^2)}. \tag{4}$$

Here it is convenient to introduce the notion of *edge currents* for a ground plane of finite width w_g.

Assume that the fringing magnetic flux that wraps the ground plane in a microstrip geometry is produced by current filaments ΔI_1 and ΔI_2 placed at the points $y = \pm w_g/2$, parallel to the signal current. These edge currents correspond to the total current in the "tails" distributed along $|y| > w_g/2$ for the infinitely wide case [19]. They are found by integrating the corresponding surface current density as

$$\begin{aligned}\Delta I_{1,2} &= \int_{w_g/2}^{+\infty} (H_y^+ + H_y^-)dy = \frac{I_S \cdot h}{\pi} \cdot \arctan\left(\frac{y}{h}\right)\Big|_{w_g/2}^{+\infty} \\ &= \frac{I_S}{\pi} \cdot \left(\frac{\pi}{2} - \arctan\left(\frac{w_g}{2h}\right)\right).\end{aligned} \tag{5}$$

For small ratios $\frac{h}{w_g} \ll 1$, that is, when the ground plane is substantially wide as compared to the height of the transmission line, the edge currents are approximately

$$\Delta I = \Delta I_{1,2} \approx \frac{I}{\pi} \cdot \frac{2h}{w_g}. \tag{6}$$

The current on the ground plane of finite size is

$$I_g = \int_{-w_g/2}^{+w_g/2} (H_y^+ + H_y^-)dy = \frac{2I}{\pi} \cdot \arctan\left(\frac{w_g}{2h}\right). \tag{7}$$

There is a current balance in the geometry,

$$I_S + I_g + 2\Delta I = 0. \tag{8}$$

However, in reality, the signal trace is of non-zero width w_s, so this is not a filament current. Though the realistic distribution of the current on the signal trace is not even, let us assume in the first-order approximation that the current density in the strip is distributed evenly [40, 42, 43],

$$J_S = \frac{I_S}{w_s}. \tag{9}$$

The magnetic field on the surface of the ground plane at the distance h from it is

$$H_y^{\pm} = \frac{J_S h}{2\pi} \int\limits_{-w_s/2}^{w_s/2} \frac{dy'}{(y-y')^2 + h^2}, \tag{10}$$

where y' is the point on the signal strip, and y is the point of observation on the ground plane.

The density of the current induced on the infinite ground plane is

$$J_g(y) = 2H_y = \frac{J_S h}{\pi} \int\limits_{-w_s/2}^{w_s/2} \frac{dy'}{(y-y')^2 + h^2}. \tag{11}$$

Then the edge currents $\Delta I_1 = \Delta I_2 = \Delta I$ are found by the integration

$$\Delta I = \int\limits_{w_g/2}^{+\infty} J_g(y)dy = \frac{J_S h}{\pi} \int\limits_{w_g/2}^{+\infty} \left(\int\limits_{-w_s/2}^{w_s/2} \frac{dy'}{(y-y')^2 + h^2} \right) dy. \tag{12}$$

The finite thickness d of the ground plane might have a substantial effect on the mutual inductance under study, so it is reasonable to take it into account in the present model. Assume that the edge currents are not filaments at the very edges of the ground plane, but they are distributed with the current density J_{edge} on the surface of the rounded edges of radius $R = \frac{d}{2}$, so that

$$J_{edge} = \frac{\Delta I}{\pi R}. \tag{13}$$

The current balance (8) must still be fulfilled.

Now the flux that contribute to the mutual external inductance under study must be determined. The contour for the magnetic flux calculation is $\{x = const;\ y = 0;\ z \in (-\infty;\ -R)\}$, as is shown in Figure 3. The integration limits are then $z \in (-\infty,\ -R)$. The total magnetic flux penetrating the contour under the ground plane is

$$\Psi_\Sigma = \Psi_S + \Psi_g + 2\Psi_{edge}, \tag{14}$$

where Ψ_S is the flux produced by the current on the signal trace, Ψ_g is the flux produced by the current distributed on the finite ground plane, and $2\Psi_{edge}$ is the flux produced by the edge currents. It is easy to show

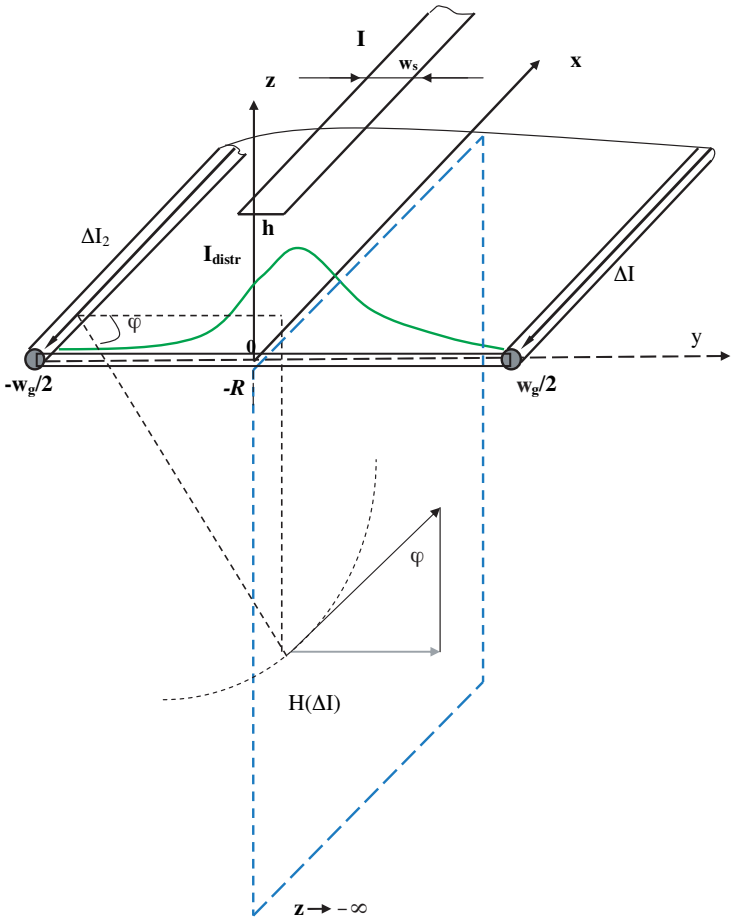

Figure 3. Currents contributing to the fringing magnetic flux wrapping the ground plane.

that the only flux responsible for the mutual external inductance is the flux produced by the edge currents. Indeed, when the ground plane is infinitely wide, flux produced by all the elemental currents completely compensates for the flux produced by the signal trace, so that there is no fringing magnetic field below the ground plane,

$$\Psi_S + \Psi_{g\infty} = 0. \tag{15}$$

However, the flux from the infinite ground plane is comprised of flux from the finite ground plane and flux from the "tails" (distributed tail currents), formed when a ground plane of finite size is cut out of the

infinite plane,

$$\Psi_S + \Psi_g + \Psi_{tails} = 0. \tag{16}$$

Due to the redistribution of the currents in the structure with finite ground planes and added lumped edge currents, the resultant flux below the ground plane is

$$\Psi = \Psi_S + \Psi_g + 2\Psi_{edge} \neq 0. \tag{17}$$

Then, this non-zero flux Ψ is obtained by subtracting (16) from (17),

$$\Psi = 2\Psi_{edge} - \Psi_{tails}. \tag{18}$$

This means that it is sufficient to calculate only the flux from the lumped edge currents and the flux from the distributed tail currents on the infinite ground plane.

The flux from the "tails" can be calculated as

$$\Psi_{tails} = \mu \cdot \int_{-\infty}^{-R} H_{y\,tails} dz, \tag{19}$$

where the magnetic field due to the "tails" is calculated through current density on the infinite ground plane as

$$H_{y\,tails} = \int_{-\infty}^{-w_g/2} \frac{J_g(y) \cdot (R-z)dy}{\pi \cdot ((R-z)^2 + y^2)}, \tag{20}$$

and $\mu = \mu_r \cdot \mu_0$ is the absolute permeability of the media ($\mu_0 = 4\pi \cdot 10^{-7}$ H/m), and R is half of the thickness of the ground plane. As further analysis using numerical calculations shows, the contribution of the tail currents is negligible compared to the contribution by the edge currents (the tail current flux is at least two orders smaller than the edge current flux).

The next step is to find the fluxes produced by the edge currents. If the edge currents are considered as filamentary, the magnetic flux through the loop in the plane $y = 0$ for $(-\infty, -R)$ beneath the ground plane will be

$$\Psi_{edge} = \frac{\mu \cdot \Delta I_{edge}}{2\pi} \cdot \int_{-\infty}^{-R} \frac{z}{z^2 + (w_g/2)^2} dz. \tag{21}$$

However, the results of the computations using this formula substantially diverge from those obtained using the other methods (e.g., Schwarz-Christoffel conformal mapping [41]), especially when the thickness of the ground plane increases, and when the width of the ground plane decreases. This suggests that the edge current should be considered as a distributed current, rather than a lumped filamentary current. Indeed, when the ground plane is comparatively narrow, the surface current induced by the signal trace on the ground plane may also appear on the opposite side of the ground plane close to the edges (Figure 4). Assume that this edge current is distributed evenly on the surface of a rounded edge (of course, this is an approximation).

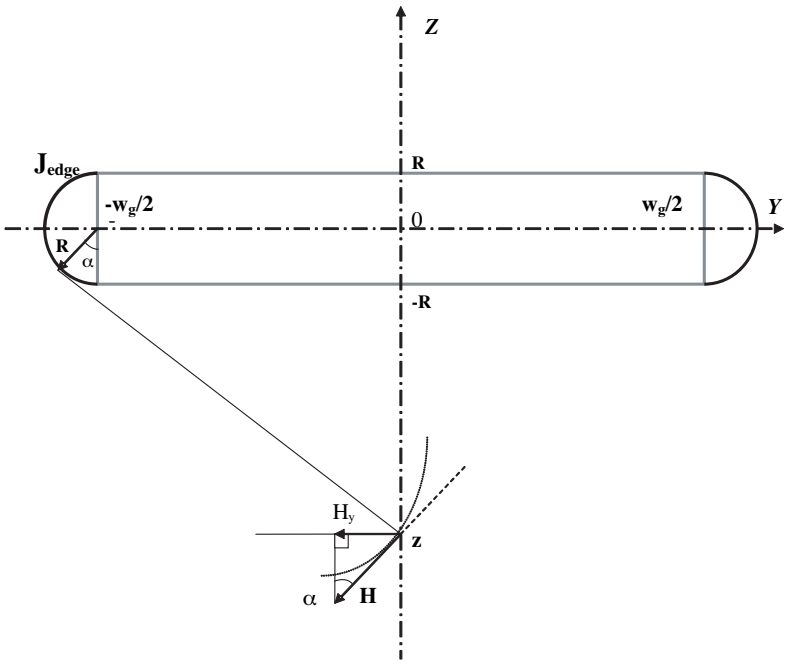

Figure 4. Calculation of the magnetic field from distributed currents on the rounded edges of a ground plane.

The contribution from any elemental current on the edge can be calculated as

$$dH_{y\,edge} = dH^{top}_{y\,edge} + dH^{bot}_{y\,edge}, \tag{22}$$

where the index "*top*" corresponds to the upper half of the ground ($0 \le z \le R$), and the index "*bot*" corresponds to the lower half of the ground plane ($-R \le z < 0$).

These elemental magnetic fields are

$$dH_{y\,edge}^{top} = \frac{J_{edge}R\left(\frac{w_g}{2}+R\sin\alpha\right)}{\pi\left(\left(\frac{w_g}{2}+R\sin\alpha\right)^2+(R\cos\alpha-z)^2\right)}d\alpha; \qquad (23)$$

$$dH_{y\,edge}^{bot} = \frac{J_{edge}R\left(\frac{w_g}{2}+R\sin\alpha\right)}{\pi\left(\left(\frac{w_g}{2}+R\sin\alpha\right)^2+(R\cos\alpha+z)^2\right)}d\alpha, \qquad (24)$$

and the resultant magnetic field is

$$H_{y\,edge} = \int_0^{\pi/2}\left(dH_{y\,edge}^{top}+dH_{y\,edge}^{bot}\right). \qquad (25)$$

Then the corresponding magnetic flux is

$$2\Psi_{edge} = 2\mu\cdot\int_{-\infty}^{-R} H_{y\,edge}dz. \qquad (26)$$

The resultant *p.u.l.* MEI of the symmetrical microstrip line is

$$M_0^{ms} = \frac{\Psi}{I_S} = \frac{2\Psi_{edge}-\Psi_{tails}}{I_S}. \qquad (27)$$

The results of computations using the above approach for a symmetrical microstrip line are presented in Figure 5. The computations were made using the mathematical software tool, *Maple 10*, that allows for direct analytical integration (both symbolic and numerical). For these graphs, the width of the trace was taken as $w_s = 0.1\,\text{mm}$, and half of the thickness of the ground plane was $R = 0.01\,\text{mm}$. As is seen in Figure 5(a), the results of the analytical integration using *Maple* and the calculations using a formula, following from the Schwarz-Christoffel (SC) conformal mapping [18, 41],

$$M_0^{ms} = \frac{\mu}{\pi}\cdot\frac{h}{w_g}, \qquad (28)$$

match very well for higher ratios $w_g/h > 3$ (discrepancy is less than 1%). When $w_g/h < 3$, there is a discrepancy between the results based on the SC conformal mapping and the proposed method, as is shown in

Figure 5(b). Figure 5(c) demonstrates that for the microstrip geometry the two curves for the mutual inductance versus the parameter w_g/h almost coincide, when the "tail" flux Ψ_{tails} are taken and not taken into account. The reason is that the "tail" flux Ψ_{tails} are negligibly small compared to the flux Ψ_{edge}, produced by the lumped edge currents.

Figure 6 shows the effect of the signal trace width on the external mutual inductance in a symmetrical microstrip line. The mutual inductance increases as the signal trace becomes wider. Figure 7 demonstrates how the ground plane thickness affects the mutual

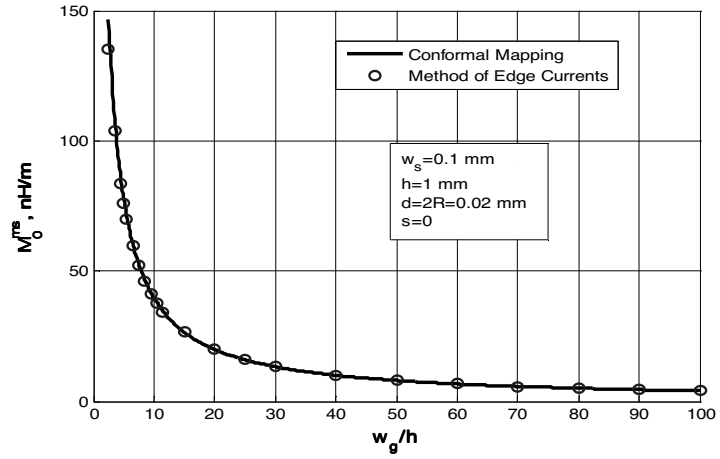

(a)

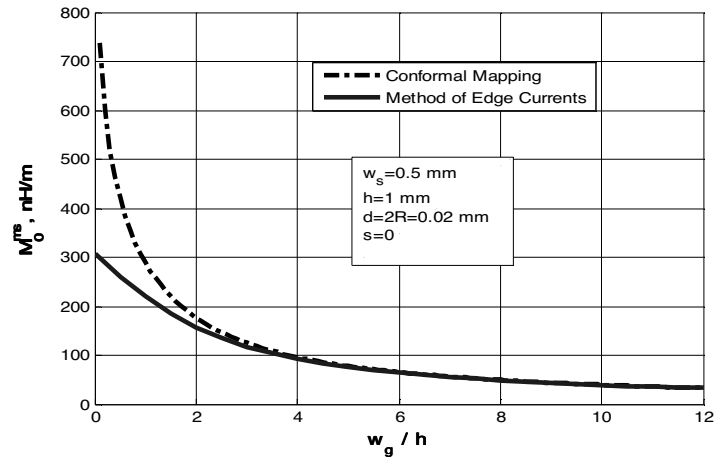

(b)

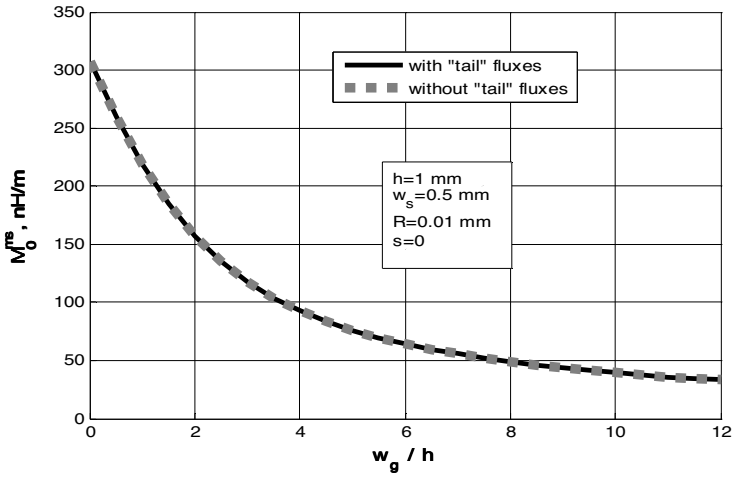

(c)

Figure 5. Mutual external inductance associated with the fringing magnetic fields wrapping the ground plane for a centered microstrip geometry: (a) at larger ratios w_g/h; (b) at smaller ratios w_g/h; (c) with and without the "tail current" flux accounted for.

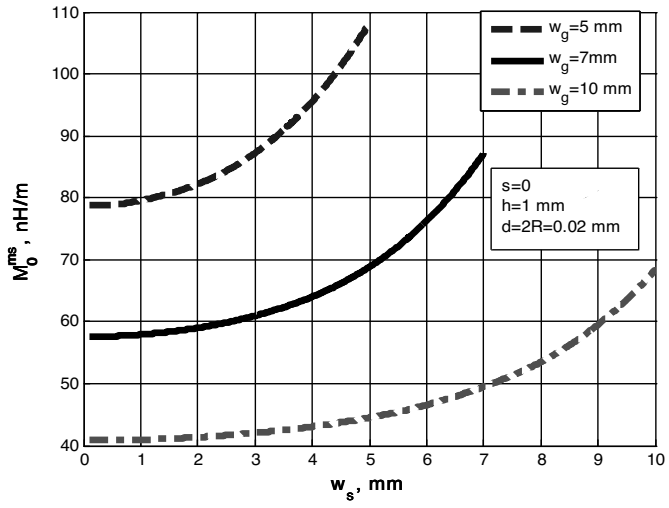

Figure 6. Mutual external inductance in a microstrip line with a centered signal trace versus width of the signal trace w_s for different widths of the ground plane.

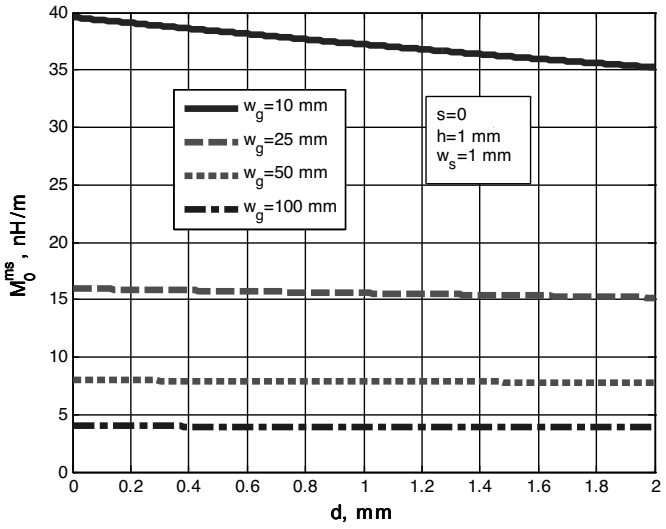

Figure 7. Mutual external inductance in a symmetrical microstrip line with a centered signal trace versus thickness of the ground plane d for different widths of the ground plane.

inductance under consideration: when the ground plane is wide enough, the effect of the ground plane thickness is negligible; and when the ground plane is narrow, the thickness of the ground plane leads to some decrease in external mutual inductance.

3. ASYMMETRICAL MICROSTRIP STRUCTURE

Let the signal trace of a microstrip line be shifted from the center of the ground plane at the distance $\Delta y = s$, as is shown in Figure 8.

Also assume that the signal trace is of a non-zero width w_1, and the surface current density on it is the same as (9). Then, taking into account the offset s, the surface current induced on the ground plane is

$$J_g(s,y) = 2H_y^+ = \frac{J_S h}{\pi} \int\limits_{s-w_s/2}^{s+w_s/2} \frac{dy'}{(y-y')^2 + h^2}, \tag{29}$$

where y' is the point on the signal trace, and y is the point of

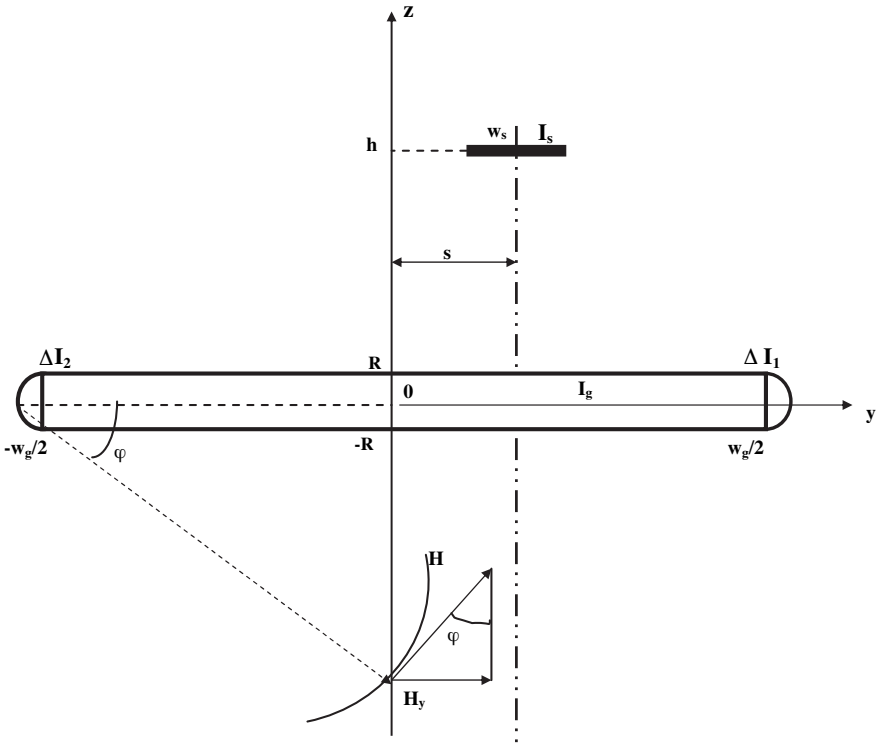

Figure 8. Application of image theory for the mutual inductance extraction in the asymmetrical microstrip case.

observation on the ground plane. The edge currents then are

$$\Delta I_1(s) = \int\limits_{w_g/2}^{+\infty} J_g(s,y)dy; \quad \Delta I_2(s) = \int\limits_{-\infty}^{-w_g/2} J_g(s,y)dy. \qquad (30)$$

If the signal trace is a filamentary current, then the ground plane current density is

$$J_g(s,y) = \frac{I_S}{\pi} \cdot \frac{h}{h^2 + (y-s)^2}, \qquad (31)$$

and the edge currents can be calculated as

$$\begin{aligned}\Delta I_1 &= \frac{I_S}{\pi}\cdot\left(\frac{\pi}{2}-\arctan\left(\frac{w_g-2s}{2h}\right)\right);\\ \Delta I_2 &= \frac{I_S}{\pi}\cdot\left(\frac{\pi}{2}-\arctan\left(\frac{w_g+2s}{2h}\right)\right).\end{aligned} \tag{32}$$

If $s=0$, these currents are equal. But in the general case of a non-zero s they are not equal. If they are distributed approximately evenly on the ground plane edges of radius R, then the corresponding current densities are calculated as

$$J_{edge\,1,2}(s)=\frac{\Delta I_{1,2}(s)}{\pi R}. \tag{33}$$

The magnetic field from the current tails of the infinite ground plane is

$$\begin{aligned}H_{ytail1} &= \int\limits_{-w_g/2}^{-\infty}\frac{J_g(y)\cdot z dy}{2\pi\cdot(z^2+y^2)};\\ H_{ytail2} &= \int\limits_{-\infty}^{-w_g/2}\frac{J_g(y)\cdot z dy}{2\pi\cdot(z^2+y^2)}.\end{aligned} \tag{34}$$

The magnetic field from the edge currents is calculated as before, but depends on the offset s and is different for the right and left edge currents.

$$\begin{aligned}H^{top}_{y\,edge\,1,2} &= \int\limits_0^{\pi/2}\frac{J_{edge\,1,2}R\cdot\left(\frac{w_g}{2}+R\sin\alpha\right)}{2\pi\left(\left(\frac{w_g}{2}+R\sin\alpha\right)^2+(R\cos\alpha-z)^2\right)}d\alpha;\\ H^{bot}_{y\,edge\,1,2} &= \int\limits_0^{\pi/2}\frac{J_{edge\,1,2}R\cdot\left(\frac{w_g}{2}+R\sin\alpha\right)}{2\pi\left(\left(\frac{w_g}{2}+R\sin\alpha\right)^2+(R\cos\alpha+z)^2\right)}d\alpha.\end{aligned} \tag{35}$$

Then the corresponding magnetic flux from the tails and from the edge currents are

$$\Psi_{tails}\;=\;\mu\cdot\left(\int\limits_{-\infty}^{-R}H_{ytail1}dz+\int\limits_{-\infty}^{-R}H_{ytail2}dz\right), \tag{36}$$

$$\Psi_{edges} = \mu \cdot \left(\int_{-\infty}^{-R} H_{y\,edge\,1} dz + \int_{-\infty}^{-R} H_{y\,edge\,2} dz \right). \tag{37}$$

The *p.u.l.* MEI of the asymmetrical microstrip is then

$$M^{ms}(s) = \frac{\Psi_{edges} - \Psi_{tails}}{I_S}. \tag{38}$$

The analytical results obtained using the proposed MEC approach are presented in Figures 9(a), (b) and 10(a), (b). Mutual inductance in a microstrip line is shown versus the normalized offset (s/w_g) for a signal trace from the center. In the computations shown in Figure 9(a), the ground plane width is $w_g = 10\,\text{mm}$, the height of the signal trace with respect to the ground plane is $h = 1\,\text{mm}$ (the ratio $w_g/h = 10$), the width of the signal trace is $w_s = 1\,\text{mm}$ (the ratio $w_s/h = 1$), and the thickness of the ground plane is $d = 2R = 0.02\,\text{mm}$.

In Figure 9(b), the width of the ground plane is $w_g = 100\,\text{mm}$, so that the ratio $w_g/h = 100$. The results are compared with those obtained using the SC conformal mapping approach [41],

$$M_s^{ms} = \frac{\mu}{2\pi} \cdot \ln \left| 2\left(\frac{s+jh}{w_g}\right) + \sqrt{4\left(\frac{s+jh}{w_g}\right)^2 - 1} \right|, \tag{39}$$

and the approximation function in [24],

$$M_s^{ms} \approx \frac{\mu}{\pi} \cdot \frac{h}{w_g} \cdot \frac{1}{\sqrt{1 - 4\left(1 - 2\frac{h}{w_g}\right)\left(\frac{s}{w_g}\right)^2}}, \tag{40}$$

as well as the mutual inductance for a trace under the very edge of the ground plane $|y| = s = w_g/2,\ z = -h$, as in [16],

$$M_{edge}^{ms} \approx \frac{\mu}{\pi} \cdot \sqrt{\frac{h}{2w_g}}. \tag{41}$$

The value of M_0^{ms} (at $s/w_g = 0$) is the same for all the graphs calculated using different approaches, as Figures 9(a) and (b) show. However, when the trace is shifted from the central position to the edge, the discrepancy between the corresponding graphs in these figures increases, especially for a wider ground plane. This can be explained by the fact that the papers [16, 24, 41] do not take into account the width

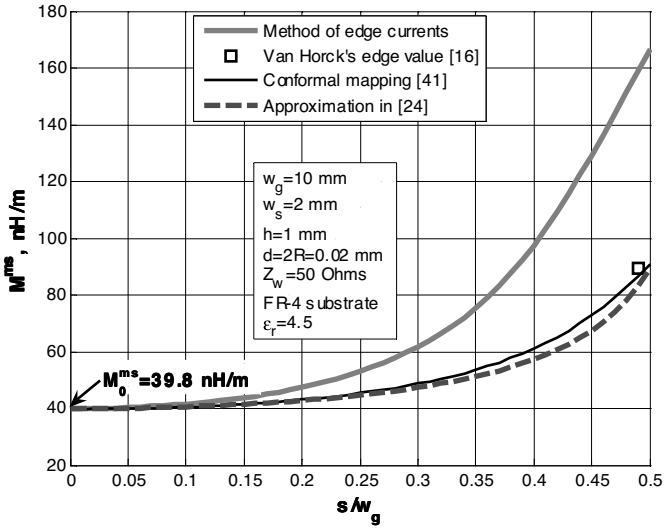

(a)

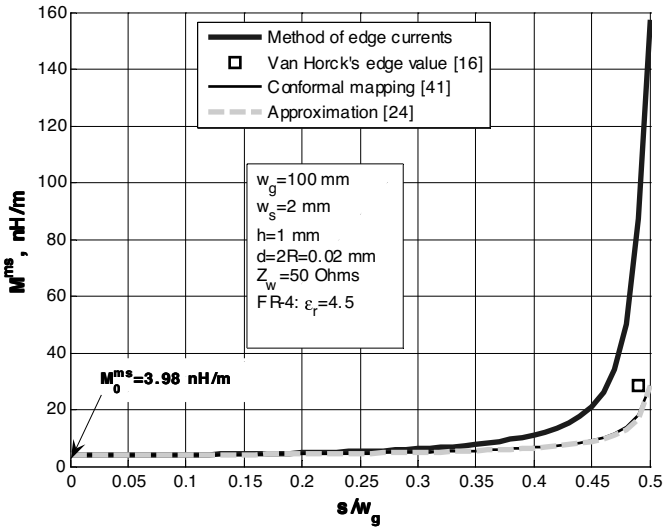

(b)

Figure 9. Mutual external inductance in a 50-Ohm microstrip line versus the normalized offset (s/w_g) for a signal trace from the center. (a) width of the ground plane is $w_g = 10\,\text{mm}$; (b) width of the ground plane is $w_g = 100\,\text{mm}$.

of the trace and the thickness of the ground plane, while the approach presented herein does. The other reason for overestimating the mutual inductance value in the MEC is concentrating an edge current close to the edge, while in reality it will be more spread under the ground plane towards the center.

Another example is shown in Figure 10. The height of the transmission line is $h = 1.143\,\text{mm}$ (45 mils), the width of the ground plane is $w_g = 100\,\text{mm}$ (corresponding to the ratio $w_g/h = 87.5$), the width of the signal trace is $w_s = 0.635\,\text{mm}$, or 25 mils (the ratio $w_s/h = 0.556$), and the thickness of the ground plane is approximately $d = 0.2\,\text{mm}$. The dielectric is FR-4 with $\varepsilon_r = 4.5$ and $\tan\delta = 0.02$.

Figure 10(a) represents only computations that use different approaches, including full-wave numerical modeling by the *CST Microwave Studio (MWS)* software. Figure 10(b) contains the comparison with some experimental results as well. These experimental results are taken from [44], and they characterize EMI produced by a microstrip structure due to the mutual inductance in terms of the relative increase of the common-mode current I_{CM} in a microstrip geometry with a signal trace shifted from the center. This increase is equivalent to the MEI normalized to its value at the center (M^{ms}/M_0^{ms}), and Figure 10(b) shows the normalized mutual inductance curves. Measurements in [44] were conducted at a frequency of 100 MHz. As is seen from Figure 10(b), the experimental results [44] are close to the calculations based on the MEC method. The analogous results that also agree well with the MEC predictions were obtained in [45] for the frequency of 350 MHz, both theoretically and experimentally.

The results of the numerical simulations using the *CST MWS* were the closest to the experimental results in [44]. The *CST MWS* software was used to calculate fringing magnetic field at different positions of magnetic probes under the ground plane. Then the MEI of interest was calculated using (3). The dependence of the magnetic field on the distance from the ground plane was obtained, and the resultant magnetic flux was calculated as an area under the curve. Initially, the computational domain in *CST MWS* was chosen as $2080\,\text{mm} \times 300\,\text{mm} \times 500\,\text{mm}$. Then the computational domain was increased to $2080\,\text{mm} \times 500\,\text{mm} \times 700\,\text{mm}$ to "capture" more of the fringing magnetic flux. In the *CST MWS* modeling it was noticed that the edge value of M increases with the increase of the computational domain (10% difference for two abovementioned computational domains). This is because more fringing magnetic flux is captured within the computational domain of a bigger volume, especially, when it increases in the y-direction and in the negative z-

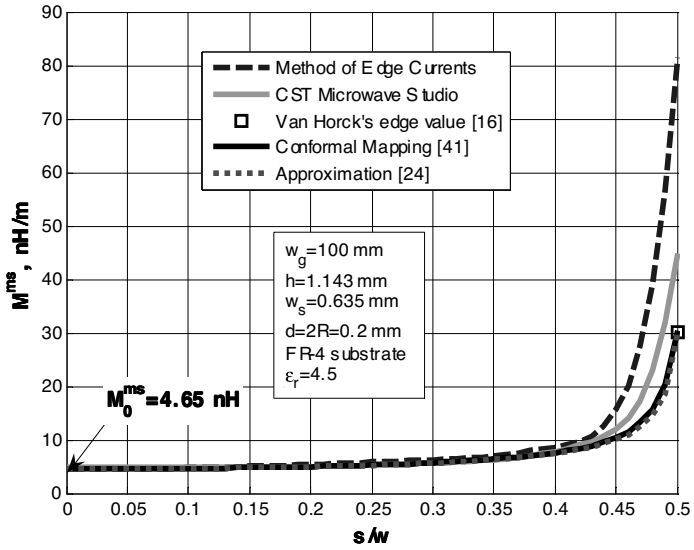

(a)

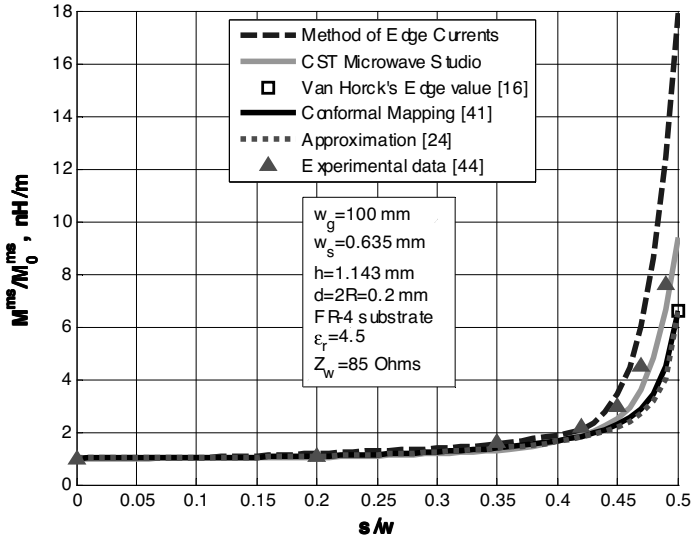

(b)

Figure 10. Mutual external inductance in a microstrip line versus offset for a signal trace from the center: (a) non-normalized, and (b) normalized and compared with experimental data in [35].

direction. Also, the calculated external inductance in the *CST MWS* is slightly higher at d.c. than at higher frequencies ($\sim$140 MHz), and this difference is around 2%. In Figures 10(a) and (b) the results for the bigger computational domain and d.c. case are shown. All the results of modeling using the *CST MWS* lie between the curve obtained by MEC, and the curves calculated using SC conformal mapping [41] and approximation in [24]. In the *CST MWS*, some of the fringing magnetic flux is absorbed by a perfectly matched layer used to limit the computational domain, so the results of computations might be underestimated. In the conformal mapping method the results are underestimated as well, since the width of the trace and thickness of the ground plane are not taken into account. The MEC gives the highest results, since the integration in this method is accomplished in an almost infinitely large space around the microstrip structure.

Figure 11 demonstrates by the arrows the magnetic field picture near the microstrip geometry.

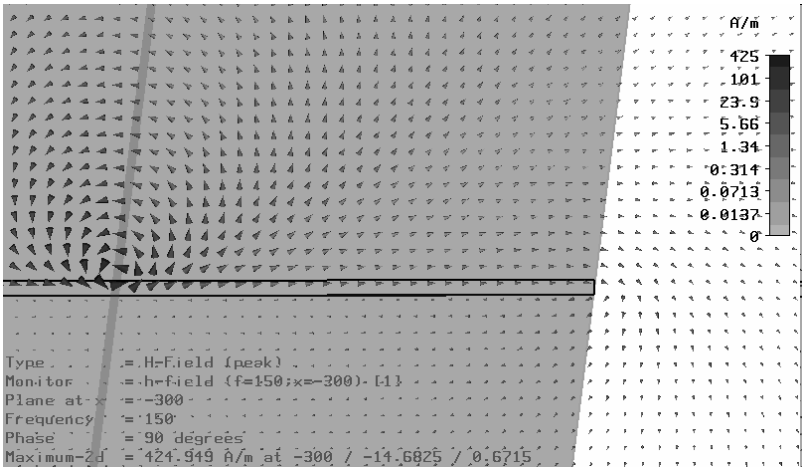

Figure 11. CST Microwave Studio modeling of magnetic field near the microstrip geometry with a finite-size ground plane.

Figure 12 shows the surface current distributions on the top and the bottom of the ground plane. These figures are obtained using the *CST MWS* software. The geometry of the structure is the same as discussed above, and the trace is shift by 15 mm from the center of the ground plane. It is seen that there are regions of enhanced surface current on the bottom of the ground plane close to the edges, and it is this current that is responsible for the mutual external inductance of interest.

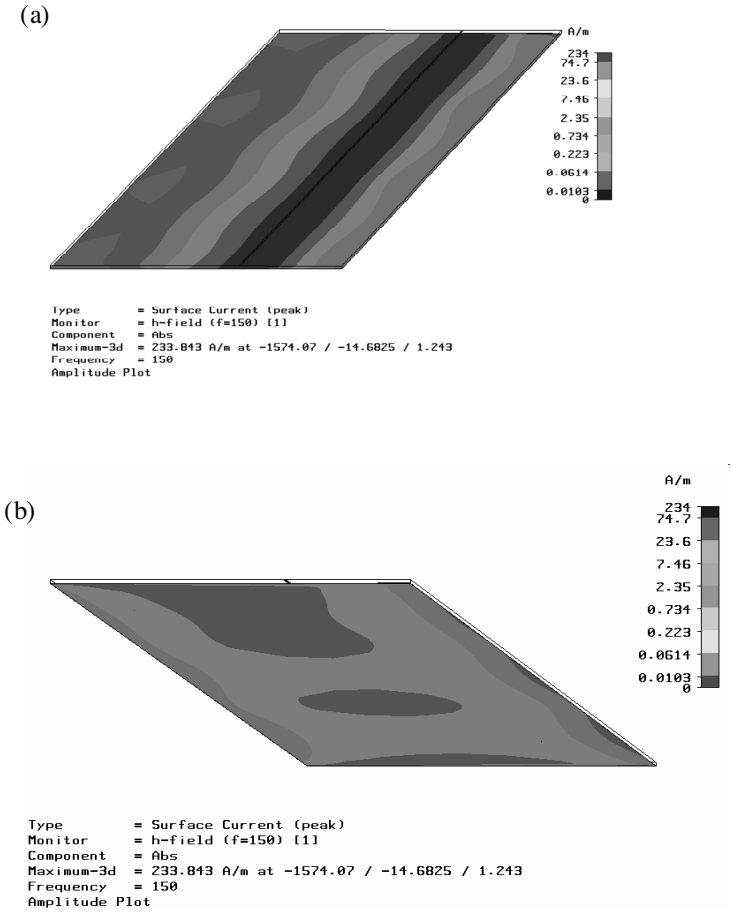

Figure 12. CST Microwave Studio modeling of surface current distributions (a) on the top, and (b) on the bottom of the ground plane in a microstrip geometry.

It should be mentioned once more that the MEC might overestimate the mutual external inductance for very narrow ground planes, since it considers edge currents distributed evenly only on the rounded edges of the ground plane. As Figure 12 shows, in reality the cut-off "tails" are redistributed on the bottom side of the ground plane, with the current density decreasing exponentially staring from the very edge towards to the center of the ground plane. This may be a direction for the further improvement of the model.

4. CONCLUSION

A *Method of Edge Currents* is proposed for calculating the mutual external inductance associated with fringing magnetic fields in microstrip structures. This method employs a quasi-static (quasi-magnetostatic and quasi-TEM) approach, image theory, superposition, and a direct magnetic field integration technique. It is shown that the residue surface currents on the tails that are cut off may be redistributed on the edges of the ground planes of finite thickness. When the ground plane is of zero thickness, these edge currents shrink and become filamentary. It is also shown that the mutual external inductance is determined mainly by the magnetic flux produced by these edge currents, while the contributions to the magnetic flux by the currents from the signal trace and the finite-size ground plane totally compensate each other. This approach has been applied to estimating mutual inductance for both symmetrical and asymmetrical microstrip lines as well. There is a good agreement with published experimental, as well as with full-wave numerical simulations.

The practically important conclusion is the following. The results of the presented computations show that, from an electromagnetic immunity (EMI) point of view, it is not acceptable to have a signal trace in a microstrip line closer than 20% of the ground plane width from the edge. This is a general and approximate recommendation for a designer. However, mutual external inductance should be evaluated for every particular case, since it depends on the offset of the signal trace from the center, on the width of the ground plane, height of the transmission line, width of the trace, and the thickness of the ground plane. The presented *Method of Edge Currents* gives the *upper limit* (worst case) of the possible mutual inductance associated with fringing magnetic fields. The practical edge values of MEI should be below the values calculated by the present method. This is beneficial for a designer. The resultant MEI is frequency-independent, since the method is limited by the quasi-static consideration, when the TEM mode is the only propagating mode in the structure.

The presented approach may also be used for the analysis of striplines and multiconductor planar transmission lines, since it is based on the superposition principle. Generalization for the multimode regime of the wave propagation is also possible.

ACKNOWLEDGMENT

CST MICROWAVE STUDIO$^{(R)}$ was used in the preparation of this paper under a collaboration agreement between UMR and CST of

America, Inc.

REFERENCES

1. Wadell, B. C., *Transmission Line Design Handbook*, Artech House, 1991.
2. Mongia, R., I. Bahl, and P. Bhartia, *RF and Microwave Coupled-Line Circuits*, Artech House, Norwood, MA, 1999.
3. Edwards, T. C. and M. B. Steer, *Foundations of Interconnect and Microstrip Design*, 3rd edition, Wiley, 2000.
4. Maloratsky, L. G., *Passive RF and Microwave Integrated Circuit Design*, Elsevier, 2004.
5. Bahl, I. and P. Bhartia, *Microwave Solid State Circuit Design*, Wiley, 2nd edition, 2003.
6. Kiang, J. F., S. M. Ali, and J. A. Kong, "Modeling of lossy microstrip lines with finite thickness," *Progress In Electromagnetics Research*, PIER 04, 85–117, 1991.
7. Takuma, T., Y. Tajima, T. Ichida, A. Z. Elsherbeni, V. Rodriguez-Pereyra, and C. E. Smith, "The effect of an air gap on the coupling between two planar microstrip lines," *Journal of The Franklin Institute*, Vol. 333, No. 2, 201–223, March 1996.
8. Watanabe, K. and K. Yasumoto, "Coupled-mode analysis of coupled microstrip transmission lines using a singular perturbation technique," *Progress In Electromagnetics Research*, PIER 25, 95–110, 2000.
9. Chai, C. C., B. K. Chung, and H. T. Chuah, "Simple time-domain expressions for prediction of cross-talk on coupled microstrip lines," *Progress In Electromagnetics Research*, PIER 39, 147–175, 2003.
10. Khalaj-Amirhosseini, M. and A. Cheldavi, "A new two-dimensional analysis of microstrip lines using rigorously coupled multi-conductor strips model," *J. of Electromagn. Waves and Appl.*, Vol. 18, No. 6, 809–825, 2004.
11. Khalaj-Amirhosseini, M., "Determination of capacitance and conductance matrices of lossy shielded coupled microstrip transmission lines," *Progress In Electromagnetics Research*, PIER 50, 267–278, 2005.
12. Arshadi, A. and A. Cheldavi, "Simple and novel model for edged microstrip line (EMTL)," *Progress In Electromagnetics Research*, PIER 65, 247–259, 2006.
13. Nashemi-Nasab and A. Cheldavi, "Coupling model of the two

orthogonal microstrip lines in two-layer PCB board (Quasi-TEM approach)," *Progress In Electromagnetics Research*, PIER 60, 153–163, 2006.

14. Khalaj-Amirhosseini, M. and A. Cheldavi, "Wideband and efficient microstrip interconnects using multi-segmented ground and open traces," *Progress In Electromagnetics Research*, PIER 55, 33–46, 2005.
15. Ymeri, H., B. Nauwelaers, K. Maex, and D. D. Roest, "New modeling approach of on-chip interconnects for RF integrated circuits in CMOS technology," *Microelectronics International*, Vol. 20, No. 3, 41–44, 2003.
16. Van Horck, F. B. M., *Electromagnetic Compatibility and Printed Circuit Boards*, CIP-Data Library, Technische Universiteit Eindhoven, 1998.
17. Leferink, F., "Inductance calculations: methods and equations," *Proc. 1995 IEEE Int. Symp. Electromagnetic Compatibility*, 16–22, Atlanta, August 14–18, 1995.
18. Hubing, T. H., T. P. Van Doren, and J. L. Drewniak, "Identifying and quantifying printed circuit board inductance," *Proc. 1994 IEEE Int. Symp. Electromagnetic Compatibility*, 205–208, Chicago, IL, USA, Aug. 1994.
19. Hockanson, D. M., J. L. Drewniak, T. H. Hubing, T. P. Van Doren, F. Sha, and C. W. Lam, "Quantifying EMI resulting from finite-impedance reference planes," *IEEE Trans. Electromagn. Compat.*, Vol. 39, No. 4, 286–297, Nov. 1997.
20. Ooi, T. H., S. Y. Tan, and H. Li, "Study of radiated emissions from PCB with narrow ground plane," *Int. Symp. Electromagnetic Compatibility*, Paper No. 20A101, 552–555, Tokyo, May 17–21, 1999.
21. Hockanson, D. M., J. L. Drewniak, T. H. Hubing, T. P. Van Doren, F. Sha, and M. Wilhelm, "Investigation of fundamental EMI source mechanisms driving common-mode radiation from printed circuit boards with attached cables," *IEEE Trans. Electromagn. Compat.*, Vol. 38, No. 4, 557–565, Nov. 1996.
22. Holloway, C. L. and G. A. Hufford, "Internal inductance and conductor loss associated with the ground plane of a microstrip line," *IEEE Trans. Electromagn. Compat.*, Vol. 39, No. 2, 73–77, May 1997.
23. Celozzi, S., G. Panariello, F.Schettino, and L. Verolino, "A general approach for the analysis of finite size PCB ground planes," *Proc. 2000 IEEE Int. Symp. Electromagnetic Compatibility*, Vol. 1, 357–362, Washington DC, Aug. 2000.

24. Leone, M., "Design expressions for the trace-to-edge common-mode inductance of a printed circuit board," *IEEE Trans. Electromagn. Compat.*, Vol. 43, No. 4, 667–670, Nov. 2001.
25. Akdagli, A., "An empirical expression for the edge extension in calculating resonant frequency of rectangular microstrip antennas with thin and thick substrates," *J. of Electromagn. Waves and Appl.*, Vol. 21, No. 9, 1247–1255, 2007.
26. Yang, F., V. Demir, D. A. Elsherbeni, and A. Z. Elsherbeni, "Enhancement of printed dipole antennas characteristics using semi-EBG ground plane," *J. of Electromagn. Waves and Appl.*, Vol. 20, No. 8, 993–1006, 2006.
27. Ataeiseresht, R., C. Ghobadi, and J. Nourinia, "A novel analysis of Minkovski fractal microstrip patch antenna," *J. of Electromagn. Waves and Appl.*, Vol. 20, No. 8, 1115–1127, 2006.
28. Shams, K. M. Z., M. Ali, and H.-S. Hwang, "A planar inductively coupled bow-tie slot antenna for WLAN applications," *J. of Electromagn. Waves and Appl.*, Vol. 20, No. 7, 861–871, 2006.
29. Kuo, L.-C., H.-R. Chuang, Y.-C. Kan, T.- C. Huang, and C.-H. Ko, "A study of planar printed dipole antennas for wireless communication applications," *J. of Electromagn. Waves and Appl.*, Vol. 21, No. 5, 637–652, 2007.
30. Ren, W., J. Y. Deng, and K. S. Chen, "Compact PCB monopole antenna for UWB applications," *J. of Electromagn. Waves and Appl.*, Vol. 21, No. 10, 1411–1420, 2007.
31. Eldek, A. A., "Numerical analysis of a small ultrawideband microstrip-fed tab monopole antenna," *Progress In Electromagnetics Research*, PIER 65, 59–69, 2006.
32. Ali, M. and S. Sanyal, "A numerical investigation of finite ground planes and reflector effects on monopole antenna factor using FDTD technique," *J. of Electromagn. Waves and Appl.*, Vol. 21, No. 10, 1379–1392, 2007.
33. Grover, H. W., *Inductance Calculations: Working Formulas and Tables*, Dover Publications, New York, NY, 1962.
34. Hoer, C. and C. Love, "Exact inductance calculations for rectangular conductors with applications to more complicated geometries," *Journal of Research of the National Bureau of Standards*, Vol. 69 C, No. 2, 127–137, 1965.
35. Maxwell, J. C., *A Treatise on Electricity and Magnetism*, 3rd edition, Oxford University Press, 1892.
36. Kaden, H., *Wirbelstroeme und Schirmung in der Nachrichtentechnik. Technische Physik in Einzeldarstellungen Herausgegeben*, von

W. Meissner (ed.), 2nd edition, 262–282, Springer-Verlag, Berlin, Germany, 1959.

37. Ruehli, A. E., "Inductance calculations in a complex integrated circuit environment," *IBM Journal on Research and Development*, Vol. 16, No. 5, 470–481, Sept. 1972.
38. Carson, J. R., "Wave propagation in overhead wires with ground return," *Bell Syst. Techn. Journal*, Vol. 5, 539–554, 1926.
39. Kobayashi, M., "Longitudinal and transverse current distributions on microstriplines and their closed-form expression," *IEEE Trans. Microwave Theory and Techn.*, Vol. 33, No. 9, 784–788, 1985.
40. Holloway, C. L. and E. F. Kuester, "Closed-form expressions for the current density on the ground plane of a microstrip line, with application to ground plane loss," *IEEE Trans. Microwave Theory and Techn.*, Vol. 43, No. 5, 1204–1207, May 1995.
41. Van Horck, F. B. M., A. P. J. van Deursen, and P. C. T. van der Laan, "Common-mode currents generated by circuits on a PCB — Measurements and transmission-line calculations," *IEEE Trans. Electromag. Compat.*, Vol. 43, No. 4, 608–617, Nov. 2001.
42. Holloway, C. L. and E. F. Kuester, "Closed-form expressions for the current densities on the ground planes of symmetric stripline structures," *IEEE Trans. on Electromagn. Compat.*, Vol. 49, No. 1, 49–57, Feb. 2007.
43. Vaidyanath, A., B. Thoroddsen, J. L. Prince, and A. C. Cangellaris, "Simultaneous switching noise: influence of plane-plane and plane-signal trace coupling," *IEEE Trans. on Advanced Packaging*, Vol. 18, No. 3, 496–502, Aug. 1995.
44. Berg, D., M. Tanaka, Y. Ji, X. Ye, J. L. Drewniak, T. H. Hubing, R. E. DuBroff, and T. P. Van Doren, "FDTD and FEM/MOM modeling of EMI resulting from a trace near a PCB edge," *Proc. IEEE Int. Symp. Electromagnetic Compatibility*, 135–140, Washington, DC, Aug. 2000.
45. Watanabe, T., O. Wada, Y. Toyota, and R. Koga, "Estimation of common-mode EMI caused by a signal line in the vicinity of ground edge on a PCB," *Proc. of IEEE Int. Symp. Electromagnetic Compatibility*, Vol. 1, 113–118, Minneapolis, MN, Aug. 2002.